

# An Integrated Approach to Understanding Vacuum Arcs

J. Norem\*

*Nano Synergy Inc., Downers Grove, IL, USA\**

Z. Insepov

*National Research Nuclear University (MEPhI), Kashira Hwy, 31, Moscow, Russia, 115409 and  
Purdue University, West Lafayette, IN, USA*

A. Hassanein

*Purdue University, West Lafayette IN, USA*

(Dated: May 18, 2022)

Almost 120 years after the isolation of vacuum arcs as a phenomenon, this field continues to be somewhat unsettled. We update our simple and general model of the vacuum arc that can incorporate all active mechanisms and aims to explain all relevant data. Our four stage model considers the trigger, plasma formation, plasma evolution and surface damage phases of the arc. Using data from failure mode analysis from solid state electronics and Atom Probe Tomography theory, we have described realistic alternatives to the Explosive Electron Emission (EEE) model for surface fracture. We show how electromigration must occur at the high current densities produced by field emission. We have identified the probable cause of shorting currents, and found that electron temperatures of  $T_e \sim 3$  eV are consistent with measurements of burn voltage and field emission thresholds. It is a requirement that any arc model must produce high  $\beta$  asperities, and we have demonstrated and explained that many active emitters with  $\beta \sim 200$ , required to explain gross arcing behavior and conditioning, can be produced at the center of arc damage. We describe how they are formed in our experiments and could be formed in higher frequency experiments with less visible damage. We have also described the conditioning process in terms of the spectrum of field enhancements, and shown how this spectrum is consistent with our earlier measurements, and describe how others could provide additional relevant data. We also describe extensions of this modeling to high power systems like tokamaks, HV transmission lines, as well as more detailed modeling of the arcs themselves. We believe this work applies directly to the designs of future high energy colliders, as well as projects like the ITER tokamak.

## I. INTRODUCTION

Arcing on surfaces occurs in many environments under many different initial conditions, such as DC, RF, vacuum or gas, pre-existing plasma, wide or narrow gap, clean or dirty conductors [1–7], for normal and superconducting systems [8], with and without strong B fields [9, 10], and ignited by high electric fields, lasers [11] or particle collisions [12]. Although vacuum arcs have been studied for over 120 years [13, 14], the field does not seem to be well understood, in that there is uncertainty over how the general mechanisms of these arcs apply to many common applications. This is unfortunate because arcing is a critical limitation on many aspects of modern technology. In this paper we suggest that the best way to improve understanding is an active dialogue between the most general models and experimental results from a wide range of environments, which we have outlined earlier [15]. We find that one of the least understood aspects of the vacuum arcs is explaining and demonstrating how arcs can produce damage, that is able to cause subsequent arcing, or more precisely, how high field enhancements are produced on damaged surfaces.

In 2001, Jüttner summarized the theoretical understanding of vacuum arcs in a review, where he argued that the understanding of arcing had not converged on a single theory applicable to a wide variety of applications, and much of the active effort in the field produced contradictory conclusions and disagreement [16]. Although common, these arcs are not well understood, since reviews do not generally consider the basic properties of electron and ion temperature and densities,  $T_e$ ,  $T_i$ ,  $n_e$  and  $n_i$ , or the asperity geometries that cause breakdown, either theoretically or experimentally. Jüttner's review summarized seven explanations of retrograde arc motion in external B fields, before advocating an eighth.

The most commonly used breakdown model is the Explosive Electron Emission (EEE) system based on studies of field emission heating of asperities [1, 3, 17]. There are problems extending this model to the widest range of experiments related to the geometries of the asperities involved. The properties of asperities that would produce the observed breakdown events are tightly constrained and well known, but these asperities are not seen experimentally. Meanwhile, other mechanisms that could trigger breakdown events are seen in a variety of environments. For example, the EEE model applies only to cathodic arcs, however similar surface fields at positive potentials (with no field emission or heating) also mechanically fracture surfaces at roughly the same local

---

\*Electronic address: norem.jim@gmail.com

fields [18, 19].

Our primary interest has been the study of mechanisms limiting the accelerating gradients of modern accelerators, since the overall cost of linear accelerator facilities is related to the gradient that can be maintained in these structures, primarily because lower gradients mean longer structures are required to produce the required performance [20]. In the design of tokamak power reactors, arcing can introduce impurities into the plasma to compromise the operation of the systems, as well as limiting the power that is available to heat the plasma to the temperature required for fusion [21]. The design of high voltage transmission lines is limited by the constraint that high surface fields can produce corona discharges that limit the operational voltage and ultimately are directly responsible for the loss of approximately 4% of the transmitted power, with the associated costs and pollution [22, 23]. Although less obvious, we find that the physics limiting integrated circuit design may also be related to surface arcing since high current densities seem to be the primary trigger in electronic component failure [24, 25] and vacuum arcs.

Surface arcs are difficult to study, and many who have been involved in this effort are interested in optimizing performance of systems rather than basic plasma physics. Problems arise since arcing can operate extremely rapidly (ns scale), the dimensions involved may be very small (a few microns or less), the dynamic range of many parameters may extend over many orders of magnitude, and the scale of surface damage from arcs and surface asperities leading to arcing may be on the order of a few nm. A further problem is the environment of experimental measurements, which must involve factors such as gas, vacuum, high fields, and unpredictable arc positions. Further complicating understanding this physics is the problem that the results of arcing experiments seem to be nonlinear due to thresholds in arc duration, available energy and other variables, so that measurable parameters seen in one experiment may not be detectable in experiments done with somewhat different parameters.

Since arcs are so important in many fields, we find that much of the R&D done has been directed at optimizing gradients or minimizing losses in specific applications, and once some arbitrary goal was reached, priorities were updated and fundamental research was reduced. Examples of this are seen in high voltage transmission lines and high-power switching systems. Nevertheless, increasing the breakdown gradients would have large economic benefits in many fields.

In order to model surface arcs and explain the behavior of basic parameters such as ion and electron temperature, density, sheath potential, as well as such as instabilities and arc motion, it seems necessary to have a simple model that can consider all the mechanisms that are necessary and sufficient at each stage of the discharge [15]. This model would need to provide a self-consistent picture of how calculations of each mechanism would operate from the initial and final conditions, and how these mecha-

nisms fit together. In principle, this exercise should be fairly straightforward, since the breakdown of a single metallic surface in a vacuum must be controlled by a small number of variables, however we find that the wide range of environments produces a variety of experimental data that is not always consistent with simple models.

This paper briefly considers how the history of vacuum arcs is compatible with a model of arcing that does not involve heating, and considers extensions of this model, highlights topics that should be studied further, describes the applications that depend on this physics, and summarizes conclusions. Since this field has been so active, we try to limit references to items that are either comprehensive, historical, or the most useful for further study.

## II. HISTORICAL DEVELOPMENT

Although an enormous number of papers have been written during the long history of surface arcing, it is interesting to isolate the most influential of these. The most complete reference on vacuum arcs is the book "Cathodic Arcs", by Andre Anders [1].

The field of vacuum arcs was isolated by Michelson and Millikan in the years 1900 to 1904. Although their work is not widely referenced today, they were able, with simple tabletop equipment, to isolate the process of vacuum arcs, measure the required electric fields required for breakdown and study the dependence on different metals [13, 14, 26]. Their results, that breakdown occurs at surface field of about 100 - 200 MV/m, agree completely with operational data from RF systems recently measured at accelerator laboratories around the world. Michelson and Millikan produced these results in air, with voltages as low as 30 V [14].

The first credible model of single surface electrical breakdown was Lord Kelvin's argument that local fields on the order of 10 GV/m would produce mechanical failure when the Maxwell stress produced by the electric field was comparable to the tensile strength of the material [27]. This prediction assumed that local surface fields could be many times higher than the average surface field, now called the field enhancement factor,

$$\beta = E_{local}/E_{average},$$

described by Alpert, accurately estimated the local field at breakdown for a range of data [7].

The work of Fowler and Nordheim in 1929 developing a quantum mechanical model of field emission that has opened up the field to numerical modeling and realistic theoretical predictions [28].

The most influential study of breakdown seems to be the study undertaken by Dyke, Trolan and co-workers, at Linfield College in Oregon in the 1950s, directed towards the optimization of intense electron sources for electron microscopes [17]. This group systematically studied breakdown of tungsten pins used as low emittance sources of electron for electron microscopes. They concluded

that heating of the metallic surface explained breakdown. This conclusion, widely confirmed, has driven much of the modeling work done subsequently, by Mesyats and others [3]. Note that their samples were micron scale pins with shapes that are not generally seen in breakdown experiments and breakdown in these experiments required pulses on the order of 10  $\mu$ sec, much longer than many RF experiments.

From about 1960, accelerator research has directed increased effort towards the problem of vacuum breakdown, in an effort to strengthen designs for high energy muon and electron linear colliders. This effort, at many accelerator labs and universities, has studied internal stresses resulting in cracks and asperities capable of causing breakdown. Studies of breakdown rates at CERN and SLAC have shown that rates can be proportional to a very high power of the electric field, as much as  $E^{30}$  although the exponents is somewhat dependent on the alloy or metal studied [29–32]. Extensive studies have also been directed at modeling the explosive electron emission numerically from a cold, pointed asperity to a hot plasma, and connecting this work to accelerator studies at CERN. This work incorporated many mechanisms such as Joule heating, atomic diffusion, plastic deformation and plasma ionization while considering realistic evolution of the asperity geometries [31].

Although the conventional wisdom seems to be that *"theoretical understanding of breakdown remains incomplete at this time, particularly with regards to the microstructural mechanisms of the field-induced ejection of matter from the structure surface that initiates the evolution of breakdown plasma, and with regards to how the mechanisms are affected by structure material conditions [31]"*, this paper argues that a realistic model of breakdown can be simple, accessible and useful.

### A. Evidence against explosive heating

While the Explosive Electron Emission model seems to be dominant, it is not universally supported [1, 16], beginning with the argument that long, narrow asperities are not generally seen in data. In the "Feynman Lectures" a simple derivation shows that, while high  $\beta$  values can be created by "fencepost" geometries, surface fields are primarily determined by the local curvature of the surface rather than the larger features of asperities [33].

Although the arcing community seem to have agreed that arcing was caused by explosive overheating, heating on a different scale was limiting the gradients of superconducting RF accelerators [8]. Field emission sources were extensively studied in the 1990's, because sensitive measurements were able to determine that field emission currents were being accelerated, heating the cavities a few mK, which was enough to limit the accelerating gradients to about 20 MV/m. These field emitters were found to have  $\beta$  values in the range  $50 < \beta < 1000$ ,

and areas  $10^{-18} < A < 10^{-9}$  m<sup>2</sup> see Fig. 12-12 in [8]. These large ranges are a significant constraint on EEE models. In addition, we find that the very sharp breakdown thresholds observed, such as breakdown rates proportional to  $E^{30}$  seem inconsistent with the random geometry of breakdown asperities overheating due to field emission currents [29].

In superconducting systems, field emitters were eventually found to be mostly manufacturing defects and metallic particulate contaminants, which are now systematically eliminated from the surface by etching the surface and high pressure water rinsing. Subsequent experiments were able to reproduce breakdown and field emission with known particulate contaminants added to the surface.

More recently, the operation and development of Atom Probe Tomography (APT) has yielded an enormous amount of data about the surfaces of small probes at *positive* fields slightly below the evaporation field of the material, which for copper, is about 30 GV/m for smooth surfaces [18, 19]. With good samples, APT can be used to produce three dimensional images of the atomic structure of the material, however there is a high probability of surface failure (flashes), resulting in lost samples and lost data. This shows that even without field emission or preexisting subsurface stresses, surfaces fail at high surface fields from Maxwell stress.

## III. BREAKDOWN WITHOUT HEATING

Since "fencepost" (unicorn horn) shaped asperities are not seen experimentally, we argue that a more general model of breakdown is needed using mechanisms where Ohmic heating is not required. We assume that breakdown occurs when Maxwell stresses are greater than the tensile stresses of the material, which occurs at surface cracks or small local radii [15]. These processes occur in a wide variety of well studied environments.

In this model the lifecycle of the arc as divided into four parts: trigger, plasma ionization, plasma evolution, and surface damage. The process occurs in four stages: 1) surface fields, measured from field emission, are high enough so that Maxwell stresses will be comparable to tensile strength causing surface failure [27], 2) field emission ionizes the surface material, producing an positively charged ion cloud near a field emitter that will increase the field on the emitter [37], 3) an unstable, non-Debye plasma is maintained by field emission and self-sputtering [38, 39], and, 4) surface damage is caused by Maxwell stresses, thermal gradients, and surface tension on the liquid metal surface.[15, 42, 43]

Our model is primarily based on data taken at 805 MHz with and without 3 T co-linear B fields, done as part of the Fermilab contribution to the Muon Accelerator Project, during 2001 - 2012 [9, 15].

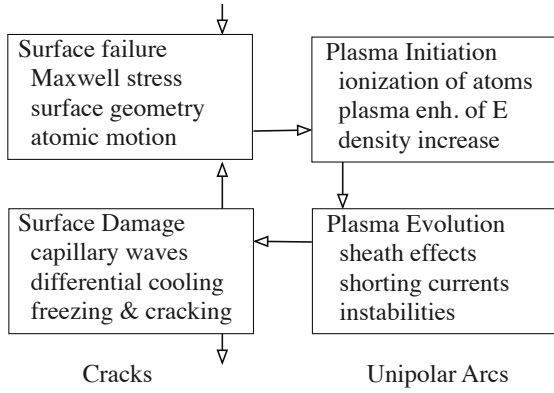


FIG. 1: Vacuum arc development involves 4 stages. We consider processes that seem dominant at different stages of the development of the arc, and find that under continued operation the arc follows a life-cycle, where damage from one breakdown event is very likely to produce another. We also find that cracks due to differential cooling and unipolar arc physics explain much of the experimental data we see.

### A. Triggers

We assume that high Maxwell tensile stresses mechanically break the surface, producing a local cloud of neutral atoms close to the asperity, which continues to field emit. The parameters of breakdown events obtained in breakdown studies at 805 MHz, are shown in Fig. 2 [9].

Following Lord Kelvin, this model assumes that triggers are due to mechanical failure of the surface due to Maxwell stresses comparable to the tensile strength and the high fields required are produced the corners that exist at crack junctions and other features [15, 27, 35, 36]. This mechanism does not require any surface heating but does require sharp features that should be visible in SEM images at high magnification. We see an abundance of crack junctions that should contain these sharp corners in our studies of 805 MHz copper cavities at Fermilab [15].

In experiments, the values of accelerating fields can be determined from the geometry and applied power. The local field at the breakdown location is more difficult to determine but can be measured from the dependence of field emitted current on electric field, which depends on the exponent  $n$ ,  $I_{FE} \sim E^n$ . The values of electric field for cavities and local models are shown in Fig. 3 [9].

It is a useful oversimplification to say that a surface will break down at  $E_{local} \simeq 10$  GV/m, because all real surfaces we consider are rough, possibly under stress at some level, and are not clean, the work functions  $\phi$  are not precisely known and the spectrum of field enhancements due to multiple asperities are not well known. We assume that the work function  $\phi \simeq 6$  eV, because the primary impurity present would be oxygen, which is electronegative [6]. This is shown in Fig 3. The experimental

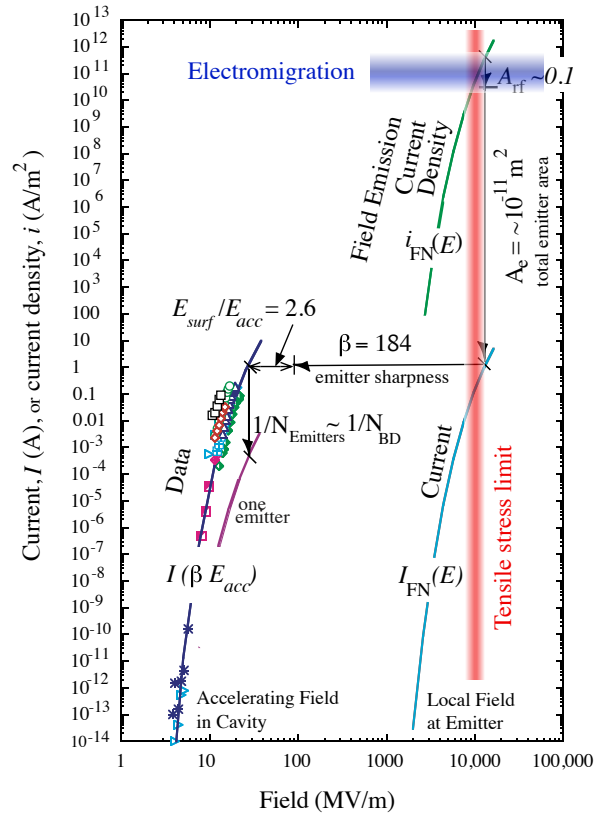


FIG. 2: Experimental data from field emission current in a cavity compared with fitted models, showing the scale of current density and electric field at the field emission sites, along with the limits that would be imposed by the material tensile strength and electromigration. [9].

parameters of the field emitting surface are limited because the only measurable quantity during high gradient operation is the exponential dependence of the field emitted current on field, requiring an estimate of the surface work function to determine the local field.

It is not possible to assume that the surface geometry of asperities is constant, since high local fields put significant stress on surface atoms. Many models assume that field enhanced diffusion explains how the field enhancement of asperities could increase with time, however electromigration (described below), which dominates diffusion under low field conditions, should maintain its relative dominance over diffusion under high stresses, as shown in experiments [24, 25].

### B. Plasma Initiation

The material removed from the surface would continue to be exposed to field emission, which would ionize it. This model assumes that plasma ions are produced with very low ion temperatures and essentially confined inertially producing a low temperature plasma near the field emitter, trapping some of the electrons, but leaving a net

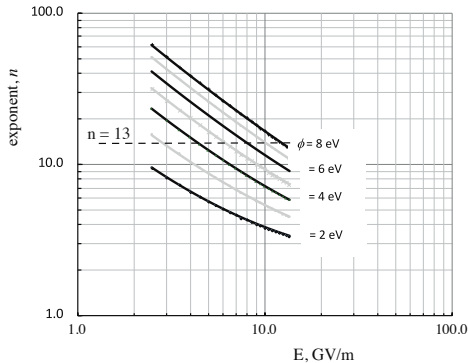


FIG. 3: The local electric field,  $E_{local}$ , can be obtained from the exponent  $n$  from field emission measurements  $I \sim E^n$  and estimates of the work function  $\phi$ . Experimental data shows that  $n \sim 14$  for radiation levels and  $n \sim 13$  for field emission.[9]

positive charge. The resulting sheath potential (and image charge) increases the field on the field emitter and confines the plasma close to the surface. Field emission maintains the plasma electrons [37]. Self-sputtering from plasma ions maintains the ion density [38], Image charges provide the charge to stick the plasma to the surface. And the density rises until the plasma becomes non-linear (non-Debye) [39].

PIC codes show that the initial plasma temperature, both  $T_e$  and  $T_i$  is cool, only a few eV, however the sheath potential between the plasma and the walls can be significantly higher than the plasma temperature. This relationship persists as the density increases and the system eventually becomes non-Debye [39].

Failures of metallic samples in Atom Probe Tomography Systems, where visible flashes are seen without the presence of field emitted electrons imply that field emission is not necessary to produce a plasma [18, 19].

### C. Plasma Evolution

We assume that the plasma produced in arcs is a unipolar arc, first described by Robson and Thoneman [45]. in 1959, and later by Schwirzke [44], Anders and Jüttner [1, 16]. The arcs are dense, unstable and frequently in motion. There is an extensive literature on these arcs, the damage they produce and their complex behavior.

The properties of unipolar arcs depend primarily on the plasma density, which can be high enough to make the plasma non-Debye, which occurs at around  $6 \times 10^{26} \text{ m}^{-3}$ , see Fig 3.48 in ref [1] and [40]. The arc properties are strongly dependent on the plasma sheath [39, 41], particularly ion self sputtering at high temperatures and high tensile stresses. When combined with other existing data on arc behavior, modeling using PIC and MD

codes, see Fig 4, has shown that densities in this range can explain the gross features of the Debye lengths, burn voltages (sheath potentials) and other plasma properties measured experimentally.

In this example, MD was used to evaluate the local equilibrium electron densities produced when electrons, which move much faster than ions, leave the plasma boundary, producing the sheath depends primarily on the electron temperature and ion density. Calculations of the sheath of non-Debye plasmas at high densities have shown that electron temperatures,  $T_e \sim 3 \text{ eV}$  and ion temperatures less than this would be consistent with experimental data on plasma density and burn voltages of 23 V, seen experimentally [15, 39] and Table B8 of Ref [1]. The calculations predict that the surface electric field produced in the sheath would be on the order of  $E > 7 \times 10^9 \text{ V/m}$ , sufficient to produce significant field emission from flat surfaces without any field enhancement. These currents would also be sufficient to short out the driving field and absorb all the electromagnetic energy in the system.

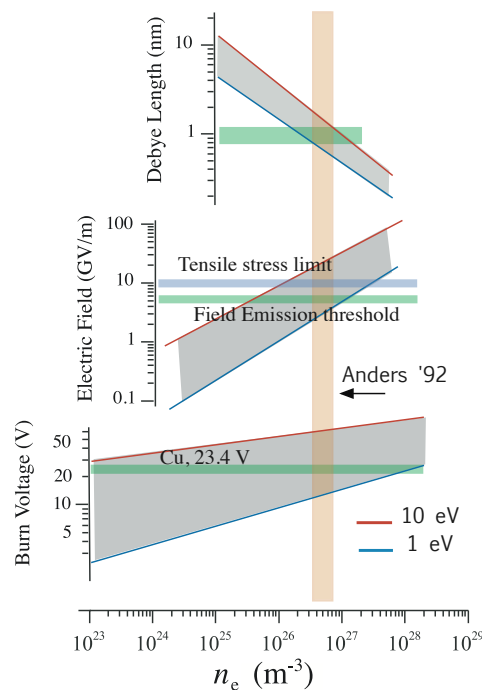


FIG. 4: The interaction between measured properties, (surface field and burn voltage) and electron temperature  $T_e$  and density,  $n_e$  from sheath calculations. [39, 40]

We can also argue that the combination of plasma pressure, Maxwell stresses and surface tension would produce a turbulent liquid surface [15]. This turbulence could be a source of instability for the plasma, leading to oscillations, local quenching and plasma motion. Thus the whole surface under the arc plasma would be emitting dense field emission currents.

### D. Surface Damage

We assume that the dominant mechanisms in surface damage are surface tension, differential cooling, solidification and contraction at locations of arc and particulate damage.

Unipolar arcs leave a variety of characteristic damage structures on materials [44]. The primary mechanisms by which the plasma affects the (presumably molten) metallic surface are plasma pressure caused by ions leaving the plasma and hitting the surface, electrostatic Maxwell stresses pulling on the surface, and surface tension, which tends to locally flatten the surface. The interplay between these mechanisms is geometry dependent. Plasma pressure tends to be locally constant, however Maxwell stresses are highly dependent on the local radius of the surface, since the force is dependent on  $E^2$ , and  $E$  near an equipotential is dependent on the local radius. Surface tension, dependent on the linear dimensions involved, becomes more dominant at small dimensions, unlike pressures, which are dependent on the areas involved. In general, plasma pressure is similar to hydrostatic pressure, which does not affect the liquid surface geometry, Maxwell stresses pull on convex shapes, becoming stronger as the tips of the surface become sharper. Surface tension tries to smooth surfaces. These effects produce a turbulent surface, perhaps with small areas pulled out from the main surface.

When the plasma terminates, this turbulent surface relaxes due to surface tension and is governed by capillary waves, locally smoothing the surface [42]. At some point the liquid metal will freeze, and the surface will continue to cool, generating stress due to thermal gradients and surface contraction. This stress can be relieved if the surface fractures, and many examples of cracks produced at the center of arc damage sites are seen [15]. The cracks produced are seen in SEM images both with and without magnetic fields, and can have the field enhancements required by breakdown calculations, as seen in Fig. 5.

The production of high field enhancements is a requirement of damage models, in order to predict realistic arcing behavior and conditioning. These cracks are not the only possible mechanism producing high field enhancements, however. Systems at higher frequencies that do not see convoluted surfaces, craters or other obvious asperities may not see these crack junctions, but they should be sensitive to particulates which could be deposited and rapidly cooled, leaving small, sharp points (high  $\beta$ s on an otherwise flat surface). These particulates should be present in vary large numbers, but might require high magnifications to identify them.

## IV. DISCUSSION

There are a number of extensions and issues that should be described by any useful model of breakdown. This field has continued to be very active since Jüttner's

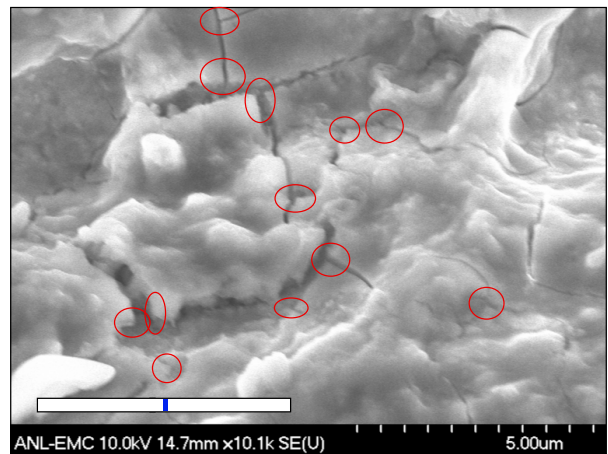


FIG. 5: Many cracks visible in SEM images of the center of an arc damage area at a magnification of 10,100x. Crack junctions where high field enhancements are expected, are noted. The widths of the cracks are caused by the thermal contraction of the material,  $\Delta x \sim x\alpha\Delta T \sim 2\%$  of the initial section, as it cools after solidifying, where  $\alpha$  is the coefficient of thermal expansion and  $\Delta T$  is the change in temperature. The overall diameter of the damage is  $\sim 500 \mu\text{m}$ , which explains the wider cracks. The blue spot is 2% of length the white line for comparison.

summary was published in 2001, however we would continue to argue that the field is not converging into a simple model of arcing that can explain behavior in many environments.

### A. Constraints on asperities

The exploding wire, or Explosive Electron Emission (EEE) model depends on high current densities and very specific thermodynamic and geometrical constraints. The primary problem seems to be due to the wide range of asperity properties seem incompatible with geometrical constraints.

Although Dyke and Trolan found that breakdown due to Ohmic heating took place in roughly  $10 \mu\text{s}$ , breakdown in X band RF structures, must occur in a few ns, which requires much higher current densities and much lower thermal conduction losses. The thermal losses can be quite high for some geometries, for example, a small right angle corner shown in Fig. 6, which could produce the required field enhancements if the radius of the corner was suitably adjusted, would have very short thermal time constant, on the order of  $10^{-14}$  s, due to the small heated volume and the large thermal losses due to small dimensions and large solid angle for heat loss.

We argue that the most likely asperity shape might be a right angle corner which can have a wider range of enhancement factors, due to the corner radius, corner size and number of asperities in one source [15]. This geometry would be consistent both with the crack junctions



we see in SEM images, where cracks actually meet at right angles, and with the small size of breakdown sites assumed in APT sample failures, described below. This geometry would be very difficult to heat to significant temperatures due to the small size of the heated volume and the large volume functioning as a thermal sink. On the other hand, the geometry is consistent with surface particulate contamination.

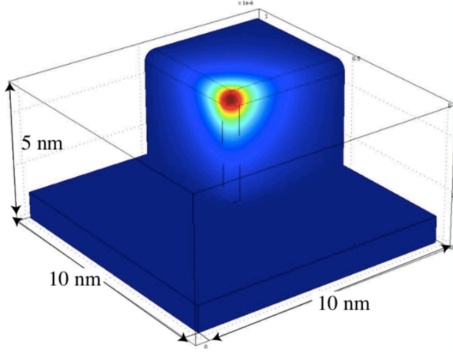


FIG. 6: The thermal time constant of small, right angle corners is  $\tau \sim 10^{-14}$  sec.

### B. Diffusion vs. Electromigration

Unlike diffusion, which is extensively modeled, electromigration has not been studied in connection with breakdown, despite some similarities in the atomic motions required. Electromigration is described by Black's equation for the Mean Time To Failure, (MTTF), [24, 25, 46, 47]

$$MTTF^{-1} = A j^2 e^{-Q/kT}$$

where  $A$  is a constant,  $j$  is the current density,  $Q$  is the activation energy for moving atoms from one place to another,  $k$  is Boltzmann's constant and  $T$  is the absolute temperature. Both electromigration and diffusion contain the Arrhenius term, essentially describing activation energy of the same atomic motions, however with electromigration the motions are driven and not random. Electromigration is the primary cause of failure in electronic components, where it easily dominates diffusion at current densities greater than  $\sim 10^{11}$  A/m<sup>2</sup>. The process is described in detail in texts on failure modes of microelectronics [24, 25].

The process of electromigration modification of surfaces has been observed using a number of techniques. Early measurements with a field emission microscope, in 1940, found that high current densities eventually formed hairlike extremities which disrupted the angular distribution of the electron emission and led to sample failure [48]. These defects are similar to those seen in semiconductor failures under high current densities [8]. They attributed this failure to electromigration.

SEM images of high currents drawn through gold surfaces in a gap have been produced at Delft showing a video of the surface being modified and eventually shorted by the electrodes. [49].

### C. Breakdown Fields

Breakdown is defined by two fields, with  $E_{average}$  and  $E_{local} = \beta E_{average}$ , where Alpert, et. al. initially showed how  $\beta$  depended on the energy of the arc [7].

It is interesting to compare the experimental limits that have been obtained for RF and DC systems in a variety of experiments with different models that have been produced over the long history of this field. Fig. 7 shows measurements by Michelson and Millikan, Lord Kelvin, with the widely used Kilpatrick limit for RF systems, along with standard limits for transmission lines, field evaporation of solid anodes (no field emission). Alpert showed that the Kilpatrick limit can be generated from data, showing that more stored energy in a system is consistent with higher values of  $\beta$  [7]. We assume that 10 GV/m initiates breakdown and the difference between the measured surface fields and 10 GV/m defines the field enhancement. The results show that the earliest measurements are consistent with recent data and models of breakdown. Note that the 10 GV/m threshold for the local electric field for copper is only a factor of three lower than the evaporation field. Thus a slight increase in roughness ( $\sim 3$ , from electromigration or roughness) would give a significant increase in tensile stress ( $\sim 10$ ).

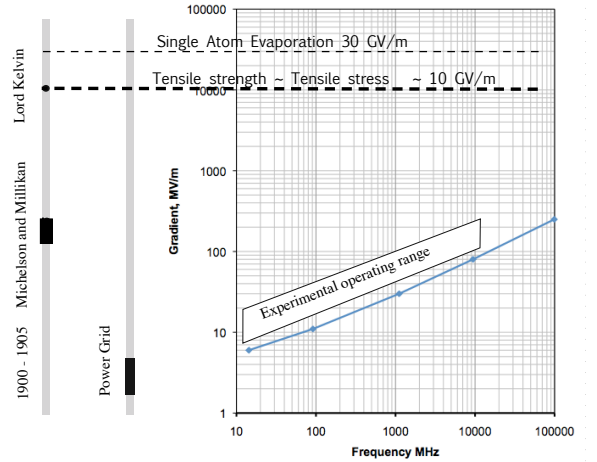


FIG. 7: RF and DC measurements of breakdown fields in different environments, along with a variety of constraints.

### D. The Conditioned Surface

The problem of conditioning illustrates some of the experimental difficulties involved with understanding arcs, with many variables and limited experimental access.

During conditioning, the surface is covered with asperities, and ones with higher local fields are expected to break down, leaving the maximum local field somewhat lower, permitting an incremental increase in average field.

Although sufficient data is available to provide a general picture, it comes from many sources and cannot be combined with precision without modeling. For example, the spectrum of enhancement factors has been measured below the breakdown threshold in a variety of environments [8, 43], field emission from conditioned cavities has been imaged with good resolution, and the field dependence of breakdown rate, has been measured [29–31]. However, these measurements have been made on different structures, at different frequencies, in programs with different goals. Detailed modeling or experimental study of mechanisms is has not been done.

If we assume that the breakdown rate is the convolution of the breakdown threshold  $t(E_{local})$  and the density distribution of the local field emitters  $n(E_{local})$ , where the product  $\beta E = E_{local}$  is equal to the local field on the field emitters, then the breakdown rate is equal to,

$$BDR \sim \int n(E_{local})t(E_{local})dE_{local}.$$

Although we are unable to measure the function  $t(E_{local})$  near the breakdown threshold, it is clear that both  $n(E_{local})$  and  $t(E_{local})$  must be sharp to produce a dependence like  $BDR \sim E^{30}$  [29, 31].

Fig. 8 sketches the spectrum of enhancement factors  $n(\beta)$  below the breakdown threshold due to arc damage from previous events. The emitter density below the breakdown threshold has been measured in unconditioned systems in a number of experiments, giving  $n(\beta) \sim e^{-\beta/40}$ , [43] and Fig. 12-14 in [8]. The dependence of the breakdown rate on field has also been measured above the threshold, and  $BDR \sim E^{30}$ , implies that  $n(E) \sim E^{-30}$  above the breakdown threshold, as shown in the figure. Note that the threshold for breakdown,  $t(E_{local})$  seems to be sharp compared to the domain of  $BDR \propto E^{30}$  behavior.

Fig 9 shows a) an image of field emission from the iris of a conditioned cavity showing single emitters with resolution of  $\sim 1$  mm with a uniform distribution of asperities and, b) a photograph of a conditioned iris in this cavity. In this large, well conditioned cavity with six irises, with a total field emitting area of approximately  $0.054 \text{ m}^2$ , we estimate a total of about 4000 active asperities near the breakdown limit and a density of field emitting asperities is roughly  $70,000 \text{ m}^{-2}$ , as seen in Fig. 8a. This image implies that in a conditioned system, all active emitters have almost identical field enhancements and field emitted currents from single emitters would be roughly  $1/N_{BD} \sim 10^{-3}$ , or less, of the total field emitted current, as shown in Fig. 2.

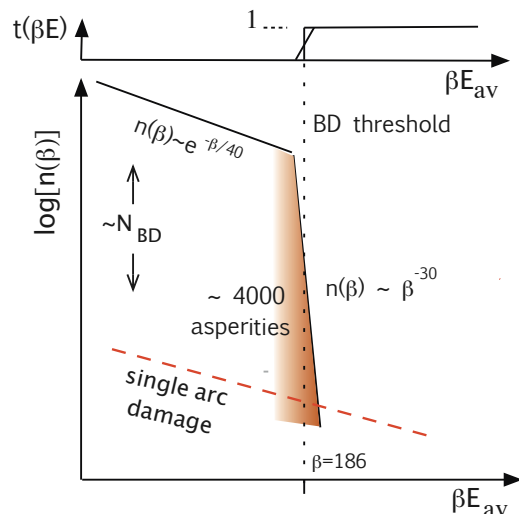


FIG. 8: The spectrum, of asperities,  $n(\beta)$ , with the threshold for breakdown  $t(\beta E)$  for a conditioned system [9]. The spectrum of asperities on the arcing surface evolves during conditioning due to creation of asperities with higher  $\beta$ s, due to single arcs. These must eventually be burned off by arcing. This is done at lower voltages to minimize generation of high  $\beta$  asperities. Not to scale.

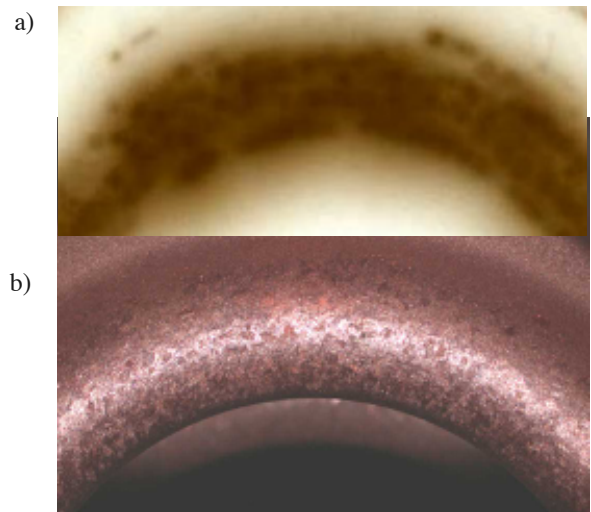


FIG. 9: The active surface in an rf cavity, showing: a) an image of field emitted beamlets from an 8 cm diameter iris in a fully conditioned cavity in a 3 T magnetic field, showing that the surface of the irises is covered in high field enhancement asperities, and the active sites are at essentially equal local field enhancements. Experimental details are presented in [9, 43], and b) an iris in the 6 cell cavity.

### E. Effects of parallel magnetic fields

There has been significant recent effort devoted to understanding the behavior of rf systems in high magnetic fields parallel to the applied electric field [9, 10].



These fields stabilize the plasma and confine electrons and plasma produced at a single location on the surface of the electrodes. This confinement has a number of consequences. It has been found in a number of experiments that two facing surfaces in an rf cavity will have damage patterns that indicate the presence of two arcs facing each other, evidently due to the effects of field emitted, accelerated beams from one arc causing another arc on the opposite face, heating the metal surface enough to cause an arc.

The surface damage produced in parallel magnetic fields tends to be radially symmetric, as one would expect from stable, radially symmetric arcs. However, the center of these circular damage sites show many cracks that seem to be the result of differential contraction and cracking, with the total crack widths roughly predicted by the degree of thermal contraction,  $\Delta r \sim \alpha R \Delta T$ , where the terms refer to the expansion constant, characteristic length, and thermal change. This completely alters the pattern of cracks which determine the effective  $\beta$ s of the damage site and the arcing threshold [15].

In focusing field emitted beams, magnetic fields also can alter the breakdown process by heating the opposing anode to a temperature at which it can trigger an arc. This has been extensively modeled and experimentally studied.

## V. COMPARISON WITH OTHER MODELS

Although other models of vacuum breakdown exist, they are less complete. As we are primarily interested in rf applications, specifically those done as part of the design of high energy linacs, we are most familiar with models generated by the CERN and collaborators, and SLAC rf groups.

The Explosive Electron Emission (EEE) model of Mesyats, assumes that the arcs are due to Joule heating of fencepost shaped asperities. As pointed out earlier, these asperities are not seen in SEM images. The EEE model does not explain surface damage and the creation of high  $\beta$  asperities in rf systems. We find that no one has shown how large numbers of these asperities could be created in the pools of liquid metal that would exist after the arc was gone [52]. In fact, we find that the surface tension tends to force the metallic pools to produce smooth surfaces if they remain liquid for a finite time. In most cases, in fact, we identify arc damage by the fact that it is locally mirror smooth, in contrast to the undamaged surface. EEE models also do not consider either electromigration or coulomb explosions as possible triggers.

Pritzkau and Siemann, showed that in cavities operating above 10 GHz, surface currents caused by rf fields heated the surface of the cavity during operation, and this cyclic heating and cooling produced internal surface stresses and visible damage, increasing rf losses and lowering the  $Q$  of the cavities [32]. The damage was pro-

duced primarily where the surface current densities were highest. While these effects seem dominant at 12 GHz, we found at 805 MHz that there was no visible damage in our cavities at high skin current locations, and there was no systematic lowering of the  $Q$  during operation. The model also predicts there will be no breakdown on the axis of a pillbox cavity where there are no surface currents, whereas in our pillbox cavity, the maximum density of breakdowns were seen on axis. Our model, which predicts and finds cracks on the surface due to very local (micron scale) thermal gradients, also predicts that the asperities produced, because they are very small and produced by tensile fracture, should be almost entirely stress free.

Mechanisms producing field enhancements on the order of 200 or higher, which were routinely seen in our data, are not a feature of either the EEE or Pritzkau and Siemann models.

## VI. APPLICATIONS

A wide range of applications provide environments similar to that of a vacuum arc, primarily sputter coating of materials [1] and switching high power currents [22]. Applications provide both an opportunity to evaluate mechanisms used in vacuum arc models, along with a large set of data that can be used to develop constraints on the mechanisms themselves. In addition, applications of vacuum arcs can provide problems where better modeling might be both economically and scientifically useful.

### A. Fusion Power Tokamaks

Tokamaks, and other systems designed to extract useful power from fusion reactions are affected by arcing and arcing mechanisms. For example, ITER, the most advanced system designed to extract usable power from fusion, involves a large toroidal plasma at high temperatures whose performance is limited by arcing in a number of ways [21, 50]. Too much surface arcing can increase the metallic contamination of the plasma, increasing losses and cooling the plasma. Likewise arcs can cool the edge plasma, making it unstable and subject to mechanically damaging disruptions. Arcing also limits the voltages that can be reached by auxiliary heating systems such as neutral beam injection, or more likely, rf heating. Calculations of responses to major disruptions have shown that single arc events might severely damage the ITER tokamak first wall.

### B. NC Accelerator cavities

Accelerators are generally designed to provide a specific particle energy, and components that limit energy

transfer to particle beams can be a significant cost constraint on their design and operation. Lowering gradients will usually require more components, larger systems and higher costs. (While plasma accelerators can, in principle, provide much higher accelerating gradients, these systems have other issues, such as transverse focusing, efficient operation and staging, that have prevented significant use of this concept.)

The limits of RF and DC gradients have been under continuous study since the 1950s, and higher gradients are now available, in part due to increased use of high frequency RF systems.

### C. SC Accelerator cavities

Although there is some duplication, the unique sensitivity of superconducting cavities to heat has increased interest in minimizing field emission in RF structures, as well as providing a very sensitive diagnostic to find and understand the role of field emitters in these systems [8]. In fact, by understanding the nature of field emitters, the field was able to develop techniques to find and eliminate them from operating cavities using etching, high pressure water rinsing and some conditioning. Many of the field emitters present on new structures were found to be particulate contamination which could be removed by high pressure rinsing, while nanoscale manufacturing defects were found to be subject to etching.

### D. HV Power Transmission Lines

A significant fraction (about 4 percent) of power transmitted on high voltage transmission lines is lost due to corona effects [22], and lower coronal losses would permit higher operating voltages with lower resistive losses. In this regulated industry, the solution to the problem seems to be to just charge more for the power. A better solution would be to explore how coatings on the wires and other surface treatments could be used to reduce this corona loss. Understanding the problem and possible solutions should precede consideration of realistic solutions.

Although corona discharges are assumed to break down in air, the highest fields are always near the conductor surface, and even if a discharge starts in air, the motion of electrons will charge the arc closest to the metallic surface positive, increasing the field on the surface, driving the arc to the surface. Experimental data shows that in corona discharges, loss currents depend on surface field like  $E^{14}$ , characteristic of field emission, see Fig. 11.4-1 of [22]. This is shown in Fig 10.

This loss is generally minimized by using large bundled cables, which reduce the electric fields on the cable surface. A better understanding of the physics of could make it possible to produce coatings that are also able to reduce coronal losses.

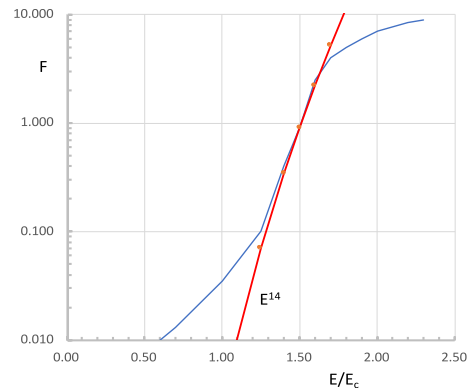


FIG. 10: Corona losses,  $F$ , on HV conductors as a function of  $E$  and the critical field  $E_c$ , showing  $I \sim E^{14}$  consistent with field emission.

### E. Atom Probe Tomography Systems

Using a process somewhat similar to a field emission microscope, Atom Probe Tomography data can be used to obtain information on mechanical failures at high fields.

Atom Probe Tomography microscope systems can produce reconstructed images of metallic probes by measuring the direction and velocity of atoms evaporated off the surface of pin shaped samples at during field evaporation at surface fields of 30 GV/m, for copper.(Appendix C of [18]), and [19]. Timing and voltage pulsing are ns scale. The samples are charged positively nevertheless it is found that metallic samples frequently "flash" or fail due to the high surface fields. Good images are obtained by insuring that the tips of the samples, on the order of 10 nm in diameter, are smooth at the scale of single atoms.

Flashing is found to occur for a number of reasons, even with samples etched to produce smooth microsurfaces. If the surface is not smooth, due to uneven etching of the sample or the effects of a grain boundary. uneven Maxwell stresses can mechanically tear the surface apart. Chemical effects due to oxides or insulating layers can also alter the surface smoothness resulting in an uneven surface, high local stresses and failure [19], p194). Surfaces in vacuum arcs cannot be smoothed in any way, and would be roughened by electromigration and other effects.

Since the goal of Atom Probe Tomography systems is to understand the material, rather than the failure mode, occasional failures are regarded as a minor inconvenience, and new samples are inserted and analyzed. Nevertheless, this results in significant volume of data on surface failure of materials at high electric fields.

## F. Electronic Components

While the environment in an integrated circuit is quite different than that of a vacuum arc, the physics of failure, involving motion of atoms from stable to unstable locations due to high current densities and electric fields, seems to be common to both [24, 25]. Current densities and electric fields in circuits are constantly increasing as component density increases and this problem will persist. Electronic failure modes are quite active as a worldwide competitive effort is underway to produce the smallest, cheapest and most reliable systems. Assuming  $10^9$  transistors / phone and  $\sim 10^9$  phones in use, each with the cheapest components possible, there is a strong motivation for this community to understand the problems of high current densities.

We assume that electromigration could have a significant role in breakdown triggers since this mechanism is a dominant source of damage in high current density electronics at densities greater than  $10^{11}$  A/m<sup>2</sup>. The geometries are not similar, however since breakdown on surfaces would allow much easier motion of surface atoms than the crystalline structure of solid state electronics.

## G. Micrometeorites, laser ablation, etc.

The range of environments that produce unipolar arcs is quite wide, based on the studies of the damage produced. For example SEM images of damage produced by micrometeorite collisions with satellites show very similar damage to the unipolar arc damage in tokamak walls, accelerator cavities and high voltage probes [12, 51]. In this case the high energy solid particle collisions generate high enough temperatures to produce plasmas, which then evolve as unipolar arcs. Likewise, high intensity lasers can also produce local plasmas on the surface of metals.

## VII. OPEN QUESTIONS

We believe that the understanding of vacuum arcs is not converging and needs a review. This review should consider a wider range of experimental data and models than are presently considered.

There are a number of issues that are unsettled and could further constrain the comparison between modeling and experiment. The arguments proposed here are not settled science. The following topics might be productive directions for study in order to generate a consensus on open issues.

We argue that roughness of surfaces combined with Coulomb explosions would explain many aspects of surface failure, however there seems to be an enormous amount of data on surface failures in APT systems that has not been systematically studied [18]. Electromigration has also not been studied in this context in spite of

its dominance over atomic diffusion, which has been exhaustively modeled as a function of temperature, stress and depth into material [24, 25].

The effects of Maxwell stress and high temperatures on self-sputtering have not been adequately documented, although loosely bound surface atoms significantly increase sputtering yields [38].

The shape of the spectrum of field enhancements described in this paper has been obtained from a variety of environments, however there should be relevant data in conditioning histories of many cavities which could be used to verify and improve the work presented here.

We need both more measurements and more modeling of basic parameters such as  $T_e, T_i, n_e, n_i$ . How do plasma pressure, Maxwell stress and surface tension determine the time evolution of the surface? Can liquid turbulence produce plasma instabilities? Can Maxwell stress explain particulate acceleration? Likewise, damage mechanisms produced by surface tension,  $\lambda$ , and gradients  $\partial T / \partial x$  are poorly studied.

Since surface damage seems difficult to see at high frequencies, perhaps a combination of higher magnifications and intermediate frequencies would produce useful data.

## VIII. CONCLUSIONS

We believe that the understanding of vacuum arcs needs a review. The field has not progressed as it should over the last 120 years, in part because modeling of individual experiments is focussed on local results, largely ignoring the vast quantity of accurate data obtained in somewhat different systems and environments. We summarized a model for breakdown that does not require heating, consisting of four stages, a trigger, plasma initiation, plasma evolution and surface damage that can be used instead of the popular EEE model [15]. We described how this model can integrate mechanisms from different fields to predict behaviors that apply to a wide range of problems such as conditioning, coronal losses, breakdown and field emission. A large range of appropriate data from other fields can provide additional constraints on modeling, helping to focus on more fundamental mechanisms.

This model provides a framework in which to evaluate all arcing phenomena, and should be a useful guide for future studies. Combining data and mechanisms from the widest class of experiments, including failure mode analysis from solid state electronics and Atom Probe Tomography theory, we have produced estimates of the spectrum of field enhancements, the field emission current from a single conditioned emitter, the electron temperature of the plasma spot, the source of shorting currents and the local threshold field for breakdown. We also find that the cracks produced by differential cooling after freezing can predict the field enhancements required by breakdown models and the cracks seen in SEM images [15]. This permits a complete understanding of the arc life-

cycle, and the details of the conditioning process. This effort has many aspects that apply to tokamaks, accelerators, solid state electronics failure modes, Atom Probe Tomography systems, and other applications.

## IX. ACKNOWLEDGEMENTS

We would like to thank the staff of Fermilab and the management of the Muon Accelerator Program who produced the facility where the experimental work we refer to was done. This work is based on experiments with 805

MHz cavities sponsored by the US/DOE, and directed at the problem of cooling diffuse beams of muons from accelerator targets. The experimental effort required a unique combination of high accelerating gradients at comparatively low frequencies and high co-linear magnetic fields, which as produced a unique environment for studying the surfaces inside conditioned rf cavities..

We would also like to thank the Center for Nanoscale Materials at Argonne National Lab. including a Hitachi SEM, an Office of Energy, Office of Science, Office of Basic Energy Sciences user facility, under Contract No DE-AC02-06CH11357.

- 
- [1] A. Anders, *Cathodic Arcs, From Fractal Spots to Energetic Condensation*, (Springer, New York, 2008), Chapter 3.
  - [2] J. M. Lafferty, *Vacuum Arcs, Theory and Applications*, (Wiley, New York, 1980).
  - [3] G. A. Mesyats and D. I. Podkurovsky, *Pulsed electrical Discharge in Vacuum* (Spinger-Verlag, Berlin, 1989).
  - [4] R. Latham, ed. *High Voltage Vacuum Insulation, Basic Concepts and Technological Practice*, (Academic Press, London, 1995).
  - [5] R. L. Boxman, P. J. Martin, D. M. Sanders, *Handbook of Vacuum Arc Science and Technology*. (Noyes Publications, Park Ridge, 1995).
  - [6] I. Brodie, and C. A. Spindt, in *Advances in Electronics and Electron Physics, Microelectronics and Microscopy, Vol 83*, Hawkes, P. W. ed. (Academic Press, New York, 1992) p 1.
  - [7] D. Alpert, D. A. Lee, E. M. Lyman and H. E. Tomaschke, *J. Vac. Sci. Technol.* **1**, 1 (1964).
  - [8] H. Padamsee, J. Knobloch, T. Hays, *RF Superconductivity for Accelerators, Second Edition*, (WileyVCH, Weinheim, 2008).
  - [9] J. Norem, V. Wu, A. Moretti, M. Popovic, Z. Qian, L. Ducas, Y. Torun, and N. Solomey, *Phys. Rev. STAB* **6**, 072001 (2003).
  - [10] A. Moretti, Z. Qian, J. Norem, Y. Torun, D. Li, and M. Zisman, *Phys. Rev. STAB* **8**, 072001 (2005).
  - [11] <https://www.jlab.org/FEL/LPC/05lpc-mao.pdf>.
  - [12] N. Meyer-Vernet, m. Maksimovic, A. Czechowski, I. Mann, I. Zouganelis, K. Goetz, M. L. Kaiser, O. C. St. Cyr, J.-L. Bougeret and S. D. Bale, *Solar Phys* (2009) 256, 463.
  - [13] R. F. Earhart, *Phil. Mag.* **1**, 147 (1901). Thesis written for A. A. Michelson.
  - [14] G. M. Hobbs, *Phil. Mag.* 10:60, 671 (1905) Thesis written for R. A. Millikan.
  - [15] Z. Insepov, J. Norem, *J. Vac. Sci. Technol. A* **31**, 011302 (2013).
  - [16] B. Jüttner, *J. of Phys. D: Appl. Phys.*, **34**, (2001) R1-3-R123.
  - [17] W. P. Dyke and J. K. Trolan, *Phys. Rev.* **89**, 799 (1953).
  - [18] M. K. Miller, *Atom Probe Tomography, Analysis at the Atomic Level*, (Kluwer, New York, 2000).
  - [19] M. K. Miller, A. Cerezo, M. G. Hetherington, G. D. W. Smith, *Atom Probe Field Ion Microscopy*, (Clarendon, Oxford, 1996).
  - [20] <https://home.cern/science/accelerators>.
  - [21] <https://www.iter.org/mach/Heating>.
  - [22] R. Lings, ed, *EPRI AC Transmission Line Reference Book - 200 kV and Above, Third Edition*, (EPRI, Palo Alto 2005).
  - [23] <https://www.instituteforenergyresearch.org/electricity-transmission/>.
  - [24] M. Ohring, *Reliability and Failure of Electronic Materials and Devices*, (Academic Press, Amsterdam, 2015).
  - [25] J. Lienig and M. Thiele, M., *Fundamentals of Electromigration Aware Integrated Circuit Design*, (Springer, Wien, 2018).
  - [26] R. A. Millikan, *The Autobiography of Robert A. Millikan*, (Prentice-Hall, New York, 1950).
  - [27] Lord Kelvin, *Phil. Mag.* **8**, 534 (1904). Also, *Mathematical and Physical Papers*, Vol. VI, Voltaic theory, Radioactivity, Electrions, Navigation and Tides, Miscellaneous, Cambridge University Press, Cambridge (1911), p. 211.
  - [28] R. H. Fowler and L. Nordheim, *Proc. Roy Soc* **A119**, 173 (1928).
  - [29] W. Wuensch, CLIC-Note-1025, CERN, (2013).
  - [30] A. D. Cahill, J. B. Rosenzweig, V. A. Dolgashev, S. G. Tantawi, S. Wethersby, *Phys. Rev.*, **21** 102002 (2018).
  - [31] W. Wuensch, A. Degiovanni, S. Calatroni, A. Korsback, F. Djurabekova, R. Rajamaki, J. Giner-Navarro, *Phys. Rev. STAB* **20** 011007 (2017).
  - [32] D. P. Pritzkau and R. H. Siemann, *Phys. Rev. STAB* **5**, 112002 (2002).
  - [33] R. Feynman, T. E. Leighton, and M. Sands, *Feynman Lectures on Physics, Vol. II*, Section 6-11, Addison Wesley, New York (1963).
  - [34] <https://home.cern/science/engineering/accelerating-radiofrequency-cavities>.
  - [35] Z. Insepov, J. H. Norem and A. Hassanein, *Phys. Rev. STAB* **7** 122001 (2004).
  - [36] Z. Insepov, J. Norem, Th. Proslier, A. Moretti D. Huang, S. Mahalingam, S. Veitzer, arXiv:1003.1736 (2010).
  - [37] Z. Insepov, J. Norem, S. Veitzer, S. Mahalingam, *Proceedings of RF2011, June 1-3, Newport R. I. AIP Conference Proceedings 1406 AIP Millville, New York (2011)*, and arXiv:1108.0861.
  - [38] Z. Insepov, J. Norem and Z. Veitzer, *Nucl. Instr. and Meth. in Phys. Res. B* **B268** (2010) 642.
  - [39] I. V. Morozov, G. E. Norman, Z. Insepov and J. Norem, *Phys. Rev. STAB*, **15** 053501 (2012).
  - [40] A. Anders, S. Anders, B. Jüttner, W. Botticher, H. Luck,

- G. Schroder, IEEE Trans. on Plas. Sci. **20** **4**, 466 (1992).
- [41] Z. Insepov, J. Norem, A. Moretti, I. V. Morozov, G. E. Norman, S. Mahalingam, S. Veitzer, Proceedings of the IPAC12 Conference, New Orleans LA, May 20-25 (2012).
  - [42] L. D. Landau and E. M. Lifshitz, Fluid Mechanics. Pergamon Press, London (1959) Chapter VII.
  - [43] A. Hassanein, Z. Insepov, J. Norem, A. Moretti, Z. Qian, A. Bross, Y. Torun, R. Rimmer, D. Li, M. Zisman, D. N. Seidman, and K. E. Yoon, Phys. Rev. STAB **9**, 062001 (2006).
  - [44] F. R. Schwirzke, IEEE Trans. Plasma Sci., **19**, No. 5, 690 (1991).
  - [45] A. E. Robson and P. C. Thonemann, Proc. Phys. Soc., **73**, 508 (1959).
  - [46] J. R. Black, IEEE Transactions on Electron Devices. IEEE. ED16 (4) (1969), p338.
  - [47] C. Z. Antoine, F. Peauger, F. Le Pimpec, Nucl. Inst. and Meth. in Phys. Res., A , **665**, 54 (2012).
  - [48] H. M. Benjamin and H. W. B. Jenkins, Proc. of Roy. Soc. **176** 262 (1940).
  - [49] <https://www.youtube.com/watch?v=tiEEfUXcRvA>, and, H.B. Heersche, , G. Lientschnig, K. Oneill, H.S.J. van der Zant and H.W. Zandbergen. Appl. Phys. Lett. **91**, 72107-1-72107-3 (2007).
  - [50] S. Kajita, N. Ohno, S. Kakamura, J. Nuc. Mat. **415** (2011) 542.
  - [51] O. N. Nikitushkina, L. I. Ivanov and A. A. Baikov. 34th Lunar and Planetary Science Conference, League City, TX, March 17-21 (2003) P1910.
  - [52] V. Dolgashev, 7th International Workshop on Mechanisms of Vacuum Arcs (MeVArc 2018), May 20-24 2018, San Juan, P. R., <https://indico.cern.ch/event/680402/>